Biochimica et Biophysica Acta 814 (1985) 111–119
Elsevier

BBA 72517

Comparison of the effects of *Anemonia* toxin II on sodium and gating currents in frog myelinated nerve

B. Neumcke, W. Schwarz * and R. Stämpfli

I. Physiologisches Institut, Universität des Saarlandes, D-6650 Homburg / Saar (F.R.G.)

(Received October 16th, 1984)

Key words: Na^+ transport; Ion channel; Gating current; Membrane-toxin interaction; Neurotoxin; (Frog nerve)

(1) Na^+ and gating currents were measured in myelinated frog nerve fibres without and in the presence of 7 μM *Anemonia* toxin II in the extracellular solution. (2) From the experiments, kinetic parameters of Na^+ currents and of gating charge displacements during ('on' response) and after ('off' response) depolarizations were determined. (3) The following parallel modifications of Na^+ currents and charge displacements by *Anemonia* toxin II were observed: the toxin reduces the maximum Na^+ permeability and the 'on' charge displacement; Na^+ activation and 'on' charge displacement become faster; Na^+ inactivation and the decline of the 'off' charge displacement with increasing pulse duration (charge immobilization) are prolonged; slow components of 'on' charge displacements are diminished. (4) The observations support the notion that the fast 'on' charge displacement is connected with the process of Na^+ activation, while Na^+ inactivation is linked to charge immobilization. Our experiments suggest that slow 'on' charge displacements during longer depolarizations are correlated with the process of Na^+ inactivation.

Introduction

Neurotoxins have become a valuable tool in the study of Na^+ channels in excitable membranes, since different types of toxins have been found which either inhibit the ion flow through Na^+ channels or modify their gating [1]. The polypeptide *Anemonia* toxin II (ATX II) from the sea anemone *Anemonia sulcata* belongs to the latter type. ATX II induces a drastic slowing of the process of Na^+ inactivation in crayfish axons [2–4], myelinated nerve [3,5–11] and in heart [12] and skeletal muscle [13] and thus prolongs action potentials. On the other hand, Na^+ activation is hardly affected.

These dissimilar effects of ATX II on the two gating processes in Na^+ channels formed the basis of our voltage-clamp experiments on myelinated frog nerve fibres. We started with an analysis of Na^+ currents, confirmed the well-known modification of Na^+ inactivation by ATX II and detected in addition a small effect of toxin on Na^+ activation. Subsequently, we studied the actions of ATX II on gating currents which arise from intramembraneous charge displacements during channel gating. By analysing ATX II-induced alterations of these displacement currents, it was possible to relate various gating current components to particular gating reactions. Specifically, ATX II accelerates the decline of gating currents after the onset of depolarizations, reduces the charge displacement and diminishes slow gating current components. Also, the immobilization of the fast charge displacement during depolarizations is slowed in ATX II. We conclude that the

* Present address: Max-Planck-Institut für Biophysik, D-6000 Frankfurt/Main 71, F.R.G.

Abbreviations: ATX II, *Anemonia* toxin II; Mops, 4-morpholinepropanesulphonic acid.

early gating current components are related to Na^+ activation while Na^+ inactivation is connected with slower current components and charge immobilization. Some of our results have been reported previously [14,15].

Methods

Single motor or sensory fibres were dissected from the tibial nerve of the frog, *Rana esculenta* [16], and a node of Ranvier was voltage-clamped at 15°C [17]. Displacements of the membrane potential from its resting value (where the steady-state Na^+ inactivation h_∞ is approx. 0.7) are denoted by V. Membrane currents were calibrated using a longitudinal axoplasm resistance determined from electrical measurements at the end of the experiment [18].

Recordings of Na^+ and gating currents were performed on different fibres first without toxin (control values) and then in the presence of ATX II in the extracellular solution. The holding potential between test pulses was set to $V_H = -20$ and -32 mV during measurements of Na^+ and gating currents, respectively. Linear components of leakage and capacity currents were compensated by an analogue circuit adjusted during a hyperpolarizing pulse starting from the holding level V_H. Na^+ and gating currents were obtained by summation of current samples recorded during and after a sequence of positive and negative test pulses of the same duration. Positive test pulses $V \leqslant 80$ mV were followed by one negative test pulse $V_H - (V - V_H)$ of the same amplitude, and positive test pulses $V \geqslant 100$ mV by two negative test pulses $V_H - (V - V_H)/2$ of half of the amplitude (see pulse programmes in Fig. 4). For measuring Na^+ currents, three sets of positive and negative test pulses were applied at an interval of 1 s, whereas gating currents were obtained from 64 of such sets taken at intervals of 0.5 s. In both cases, current samples were recorded at 10.2 μs intervals and were filtered at 25 kHz. To avoid large numbers of stored data, subsequent samples were averaged if the sampling period exceeded 1 ms.

Solutions. To block K^+ currents, the ends of the fibre were cut in a solution containing 113 mM CsCl and 7 mM NaCl, and all extracellular solutions contained 10 mM tetraethylammonium ion. Control values of Na^+ currents were recorded in K^+-free Ringer's solution containing 110 mM NaCl, 10 mM tetraethylammonium chloride, 1.8 mM $CaCl_2$ and 4 mM Mops buffer adjusted to pH 7.2 with NaOH.

Measurements of control gating currents were done in a Na^+, K^+-free solution composed of 105 mM tetramethylammonium chloride, 10 mM tetraethylammonium chloride, 1.8 mM $CaCl_2$, 300 nM tetrodotoxin and 10 mM Mops buffer titrated to pH 7.2 with tetramethylammonium hydroxide.

ATX II was obtained from Ferring Pharmaceuticals, Kiel. Before the experiment, some millilitres of 7 μM ATX II in K^+-free Ringer or in Na^+, K^+-free solution were prepared. The toxin-containing solution was perfused into the fluid pool surrounding the test node and the flow across this compartment was turned off. After a few minutes, measurements of toxin-modified Na^+ or gating currents were begun. To obtain comparable conditions, control Na^+ and gating currents were also recorded with the flow of extracellular solution stopped.

Analysis. The kinetics of Na^+ currents, $I_{Na}(t)$, from the beginning of the depolarization up to the early phase of Na^+ inactivation were fitted by the relation:

$$I_{Na}(t) = I'_{Na}(1 - \exp(-t/\tau_m))^3 \exp(-t/\tau_{h1}) \quad (1)$$

and the early and late phases of Na^+ inactivation until the end of the 11.5 ms test pulses separately by:

$$I_{Na}(t) = A_1 \exp(-t/\tau_{h1}) + A_2 \exp(-t/\tau_{h2}) + B \quad (2)$$

with the least-squares method of Gauss.

The parameter I'_{Na} in Eqn. 1 is the intercept of the extrapolated early inactivation phase with the ordinate. In the m^3h formulation of Na^+ activation and inactivation, this zero-time current is proportional to the Na^+ permeability:

$$P'_{Na} = \bar{P}_{Na} m_\infty^3 h_0 \quad (3)$$

which would be attained when Na^+ activation had reached the steady-state value m_∞ and if Na^+ inactivation were to remain at its initial value h_0 [19]. Under control conditions, the steady-state

Na^+ current, B, in Eqn. 2 was smaller than 0.5% of $A_1 + A_2$, the sum of the amplitudes of early and late phases of Na^+ inactivation. In the presence of 7 μM ATX II, the current B is larger and reaches values up to 0.22 ($A_1 + A_2$), (compare Fig. 1).

The measured gating currents were integrated numerically during the test pulse ('on' response) and after repolarization to the holding potential ('off' response) to obtain the charge displacements $Q_{on}(t)$ and $Q_{off}(t)$, respectively. Both $Q(t)$ values were then fitted by the expression:

$$Q(t) = Q(1 - \exp(-t/\tau)) + a \cdot t \qquad (4)$$

which describes a fast exponential charge transfer followed by a slower contribution $a \cdot t$ linearly increasing with time t. The second term was introduced to account for slowly decreasing components of gating currents as well as for a slowly changing or steady asymmetry of ionic currents. We have preferred Eqn. 4 to a fit with two exponentials, because two time constants can be resolved only for the 'on' response at large depolarizations [20].

Due to immobilization of mobile charges during depolarizing test pulses, the fast charge displacement, Q_{off}, of the 'off' response, is smaller than the corresponding quantity, Q_{on}, of the 'on' response [21]. The time course of this charge immobilization was described by a time constant which was obtained by fitting an exponential function to the values of the relative charge $|Q_{off}/Q_{on}|$ at various pulse durations which are shown in Fig. 8.

Results

Na^+ currents

The effects of 7 μM ATX II on the amplitude and kinetics of Na^+ currents are illustrated in Fig. 1. The currents at various depolarizations are shown on an expanded time scale in parts A and C and the continuation of the currents after their peak values in parts B and D. The most striking toxin effects are seen in the inactivating phases of the Na^+ currents: the toxin-modified currents in part D decay much more slowly and reach a higher steady-state value than the control currents in part B. Peak Na^+ current parameters are only little affected by the toxin: the time to the peak Na^+ current is not significantly changed by ATX II and the amplitude of the peak currents is 10–20% lower in the presence of the toxin (compare the currents in Fig. 1A and C).

Time constants of Na^+ activation and inactivation as obtained by fitting Eqns. 1 and 2 to the Na^+ currents in Fig. 1 and to currents from two other fibres are plotted in Figs. 2 and 3. ATX II reduces the peak height and induces a -4 mV shift of the voltage dependence of the activation time constant τ_m (Fig. 2). Thus, there is a small but significant decrease of τ_m above 40 mV. On the other hand, the time constants τ_{h1}, τ_{h2} of the early and late phases of Na^+ inactivation (open symbols in Fig. 3A and B) are strongly increased after toxin application. As a result of these opposite changes of τ_m and τ_{h1}, τ_{h2}, the time to the peak Na^+ current is hardly affected by ATX II.

Due to the slowed Na^+ inactivation in ATX II, the toxin reduces the parameter I'_{Na} in Eqn. 1 more strongly than the peak Na^+ current. Ratios of currents I'_{Na} with and without toxin are represented as open symbols in Fig. 5 and range between 0.66 at 80 and 100 mV and 0.81 at 40 mV. The ratios of the currents, I'_{Na}, are identical to the ratios of the Na^+ permeabilities, P'_{Na}, and can be decomposed into alterations of m_∞^3 and of $\bar{P}_{Na}$ according to Eqn. 3. This yields a small shift of -4 mV for the Na^+ activation curve $m_\infty^3(V)$ leaving as major effect of ATX II a reduction of the maximum Na^+ permeability $\bar{P}_{Na}$.

Gating currents

Fig. 4 shows original records of gating currents under control conditions and in the presence of 7 μM ATX II during and after depolarizations of 40 and 100 mV. The most obvious toxin effect is the reduction in the size of the 'on' gating currents during the test pulse. Consequently, the charge displacement Q_{on} becomes smaller after toxin application. Quantitative results of this charge decline are presented in Fig. 5 in which the filled symbols denote ratios of Q_{on} values with and without ATX II at various depolarizations. When toxin-modified Q_{on} values are scaled to control values at large depolarizations, the $Q_{on}(V)$ relations in ATX II are shifted by -5 to -6 mV with respect to the control curves.

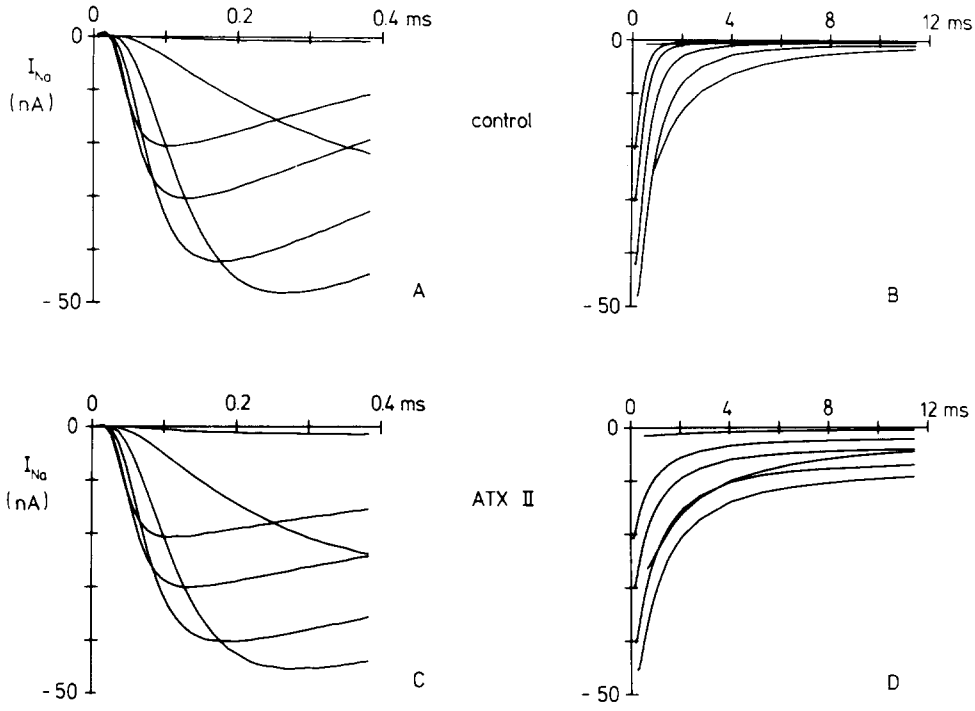

Fig. 1. Na^+ currents I_{Na} before (A, B) and during treatment with 7 μM ATX II (C, D) for depolarizations V from 20 up to 120 mV in steps of 20 mV. Parts A and C show the activation of I_{Na} on an expanded time scale, the inactivation of I_{Na} after the peak Na^+ inward current is illustrated in parts B and D. Experiment No. 7; sensory fibre; temperature, 15°C.

The toxin ATX II does not only reduce the charge displacement during the 'on' response, it also speeds up their kinetics. This feature is already visible in Fig. 4 in which the decaying phases of the 'on' gating currents at 40 and 100 mV reach the baseline at earlier times after toxin treatment. A clearer indication for the abolishment of slow 'on' gating current components by ATX II comes from a comparison of the integrated currents before and after toxin treatment. Fig. 6 shows an example and demonstrates the long-lasting increase of the control charge displacements in contrast to the more horizontal lines between 0.4

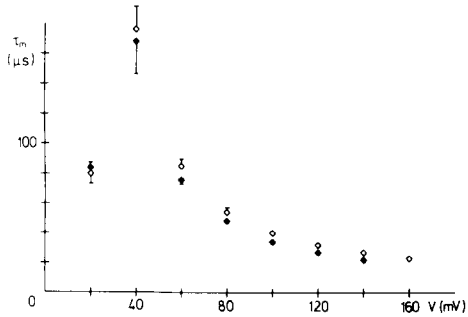

Fig. 2. Time constants τ_m of Na^+ activation at various depolarizations V before (◇) and during treatment with 7 μM ATX II (◆). Symbols show mean values from three experiments, bars indicate S.E. of mean if larger than size of symbol. Temperature, 15°C.

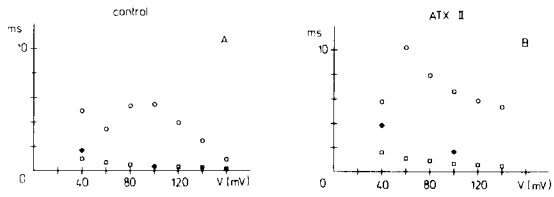

Fig. 3. Time constants of the early (□) and late (○) phases of Na^+ inactivation and of charge immobilization (◆) at various depolarizations V before (A) and during treatment with 7 μM ATX II (B). The inactivation time constants are mean values from three experiments, the immobilization time constants were obtained from the values of the relative charge in Fig. 8. Temperature, 15°C.

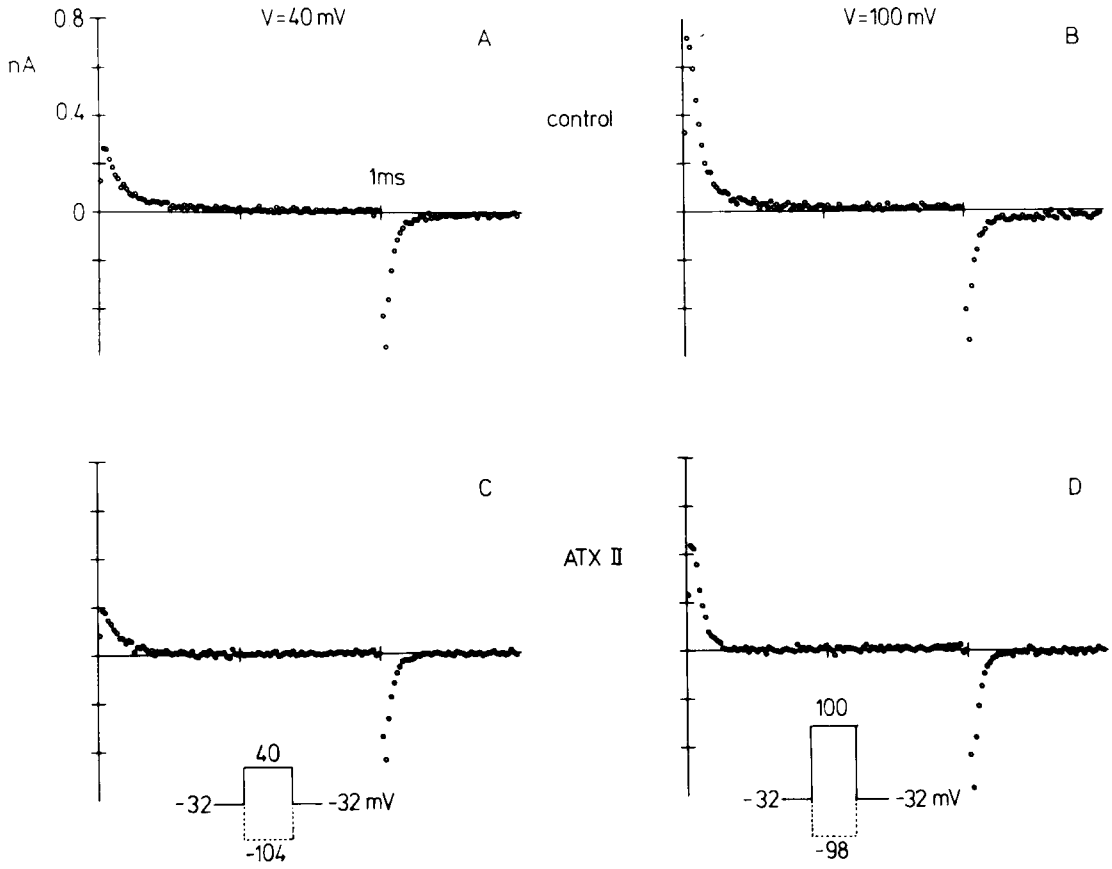

Fig. 4. Gating currents during and after 1-ms depolarizations to $V = 40$ mV (A, C) and 100 mV (B, D) before (A, B) and during treatment with 7 μM ATX II (C, D). Pulse programmes, see bottom. Units of abscissa and ordinate as indicated in (A). The corresponding fast charge displacements Q_{on} and Q_{off} in fC ($=10^{-15}$ As) and the time constants τ_{on} and τ_{off} in μs are as follows: (A) Q_{on}, 25.1; τ_{on}, 106.2; Q_{off}, −21.7; τ_{off}, 36.8. (B) Q_{on}, 48.6; τ_{on}, 69.5; Q_{off}, −19.6; τ_{off}, 36.9. (C) Q_{on}, 15.2; τ_{on}, 83.6; Q_{off}, −16.5; τ_{off}, 34.3. (D) Q_{on}, 24.6; τ_{on}, 51.2; Q_{off}, −21.2 τ_{off}, 34.2. Experiment No. 13; motor fibre; temperature, 15°C.

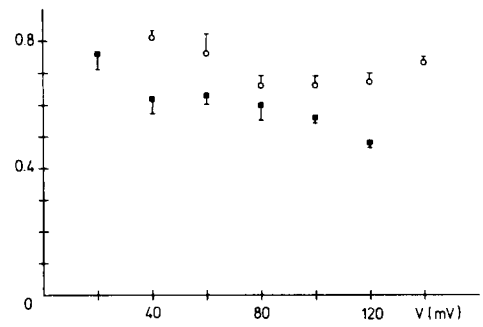

Fig. 5. Ratios of zero-time Na^+ currents I'_{Na} (○) and ratios of charge displacements Q_{on} (■) during and before treatment with 7 μM ATX II at various depolarizations. Symbols show mean values from three to seven experiments, bars indicate S.E. of mean.

and 0.5 ms in the presence of ATX II (most obvious for the high depolarizations of 100 and 120 mV).

The toxin also accelerates the fast charge transfer after the onset of depolarizations as found by fitting Eqn. 4 to the integrated 'on' gating currents. Time constants τ_{on} obtained from this fit are compiled in Fig. 7. The figure demonstrates that at various depolarizations V between 20 and 120 mV, the control values (open symbols) are always larger than the toxin-modified time constants (filled symbols). As explained in Methods, it is not possible to resolve two time constants in the kinetics of gating currents at all potentials. In cases in which the biphasic decay of the gating current is

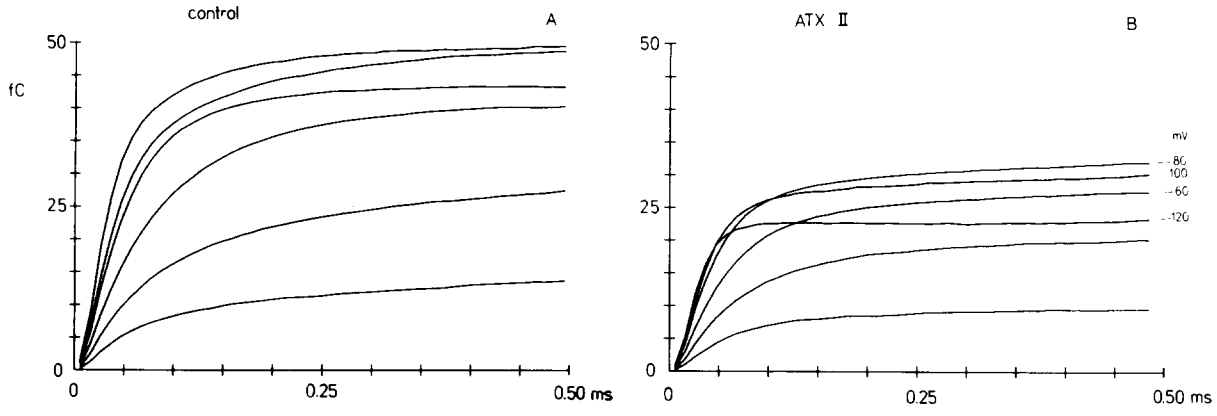

Fig. 6. Kinetics of charge displacement $Q(t)$ during depolarizations V from 20 up to 120 mV in steps of 20 mV before (A) and during treatment with 7 μM ATX II (B). Gating currents were measured in the sequence: 100, 60, 20, 40, 80 and 120 mV. Experiment No. 10, motor fibre; temperature, 15°C.

clearly visible, ATX II seems to reduce primarily the slower component (e.g., compare the 'on' responses of Fig. 4B and D). A fit with only one exponential will thus yield a smaller time constant τ_{on} in ATX II. This could account for the decreased τ_{on} values at all depolarizations.

Fig. 8A and B illustrate the effects of ATX II on the immobilization of mobile charges during pulses to $V = 40$ and 100 mV. Plotted in these figures are the ratios of the fast 'off' and 'on' charge displacements, without (open diamonds) and with ATX II (asterisks), as function of pulse duration. These relative charges decline with increasing pulse lengths, indicating a loss of fast charge displacement during prolonged depolarizations. This charge immobilization proceeds more slowly in the presence of ATX II. Time constants of the immobilization process are plotted as filled diamonds in Fig. 3 and lie between the time constants τ_{h1}, τ_{h2} of the early and late phases of Na^+ inactivation.

With increasing pulse duration, the fast 'off' charge displacement reaches a constant value. The relative charge after long depolarizations is higher in the presence of ATX II (Fig. 8). However,

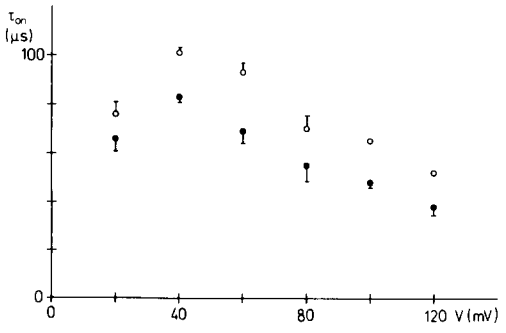

Fig. 7. Time constants τ_{on} of fast 'on' charge displacement at various depolarizations V before (○) and during treatment with 7 μM ATX II (●). Symbols show mean values from four to eight experiments, bars indicate S.E. of mean if larger than size of symbol. Temperature, 15°C.

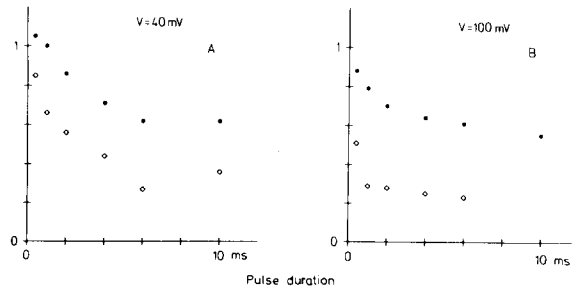

Fig. 8. Relative charge displacements $|Q_{off}/Q_{on}|$ after pulses to $V = 40$ mV (A) and 100 mV (B) versus pulse duration before (◇) and during treatment with 7 μM ATX II (*). Value ◇ in (A) at 6 ms from one single measurement, all other symbols represent mean values from three to four experiments. Temperature, 15°C.

absolute Q_{off} values after long test pulses are almost identical under control conditions and in the presence of ATX II (e.g., compare the Q_{off} values of the gating currents shown in Fig. 4B and D). Hence, the toxin does not seem to affect the fast charge displacement with resists long depolarizations.

Discussion

Our measurements of Na^+ and gating currents were performed without and in the presence of a fixed concentration of 7 μM ATX II in the extracellular solution. At this toxin concentration, the steady-state Na^+ current persisting at the end of 15-ms depolarizations has reached saturation [8]. This means that higher concentrations of ATX II do not affect additional Na^+ channels. Hence the currents recorded in 7 μM ATX II mainly originate from toxin-modified Na^+ channels.

In agreement with several previous investigations on myelinated nerve fibres [5–8], we observed a drastic slowing of Na^+ inactivation after the application of ATX II (see Fig. 1). As in normal fibres [22], the toxin-modified inactivation kinetics can be satisfactorily described as sum of two exponential functions with time constants τ_{h1} and τ_{h2}. It was reported earlier [7] that for depolarizations V between 24 and 60 mV, the time constants τ_{h1} of the early inactivation phase are hardly affected by ATX II, whereas the time constants τ_{h2} of the late phase without and with toxin exhibit opposite voltage dependencies in this potential range. Our present experiments which were extended to higher depolarizations have confirmed these features in the range from 40 to 60 mV and in addition have shown that the toxin-modified τ_{h2} values reach a maximum near 60 mV whereafter they decline at higher depolarizations (compare Fig. 3). Our τ_{h1}, τ_{h2} time constants are also in fair agreement with the results from another laboratory [8].

In our experiments, we have detected a small but significant effect of ATX II on Na^+ activation. Evidence for this comes from a change of the time constant τ_m (Fig. 2) and of the steady-state value m_∞^3 of Na^+ activation after toxin application. The two parameters τ_m and m_∞^3 were obtained from a fit of Na^+ currents by Eqn. 1 assuming independent gating processes for Na^+ activation and inactivation. If these two gating processes are coupled, alterations of Na^+ activation can already be induced by modifications of Na^+ inactivation [23]. Therefore, we have repeated the analysis of Na^+ currents under control conditions and in the presence of ATX II with the coupled gating scheme [24]:

$$C_1 \underset{b}{\overset{3a}{\rightleftharpoons}} C_2 \underset{2b}{\overset{2a}{\rightleftharpoons}} C_3 \underset{3b}{\overset{a}{\rightleftharpoons}} O \underset{d}{\overset{c}{\rightleftharpoons}} I \qquad (5)$$

Here C_1, C_2 and C_3 denote three closed Na^+ channel states before the open state O. The inactivated state I only can be reached through the open state O which implies strict coupling between Na^+ activation and inactivation. The sequence 3 : 2 : 1 of the forward and reverse activation rate constants a, b was chosen in accordance with the conventional m^3 formulation of Na^+ activation. With this gating scheme, a satisfactory description of the control Na^+ currents from the beginning of the depolarization until the early phase of Na^+ inactivation could be achieved. An attempt was then made to simulate the Na^+ currents in ATX II by varying only the inactivation rates c, d but leaving the activation rates a, b unchanged. With such changes of c and d, the slowed inactivation and the reduced I'_{Na} values could be reproduced, but the calculated peak Na^+ currents became larger and the predicted time to the peak Na^+ current longer in ATX II. Since these two changes are in conflict with our experimental results, we have to conclude that ATX II reduces the maximum Na^+ permeability and modifies the process of Na^+ activation even when it is coupled to Na^+ inactivation.

The toxin ATX II does not only modify Na^+ currents, it also affects the amplitude and kinetics of gating currents (compare Fig. 4). These gating current measurements were performed in the presence of 300 nM tetrodotoxin to abolish any ion flow through Na^+ channels. The toxin ATX II was added after control gating currents had been recorded and thus affects Na^+ channels even after tetrodotoxin blockage. Hence, ATX II and tetrodotoxin bind to different receptors.

The effects of ATX II on gating currents are comparable to those of scorpion toxins [25,26]:

both toxins reduce the 'on' charge displacements during depolarizing test pulses and abolish slower components of the 'on' response. Also, the charge immobilization during depolarization proceeds much more slowly or even vanishes after toxin treatments. The degree of these immobilization changes seems to be correlated with the strength of modification of Na^+ inactivation: a complete destruction of Na^+ inactivation in squid giant axons by pronase removes charge immobilization totally [27].

There are also some similarities between the actions of ATX II and local anaesthetics on gating currents in myelinated frog nerve fibres and in squid giant axons. Benzocaine like ATX II does not affect the fast 'off' charge displacement that persists in frog nerve after long depolarizing test pulses [28]. Also, in squid giant axons, neutral and permanently charged local anaesthetics have no effect on the non-inactivating component of the gating currents [29]. The inactivating component, on the other hand, seems to be very liable to various pharmacological treatments.

Our experiments reveal the following parallel modifications of Na^+ and gating currents by ATX II: the toxin reduces the time constants of Na^+ activation (Fig. 2) and of the fast 'on' charge displacement (Fig. 7). On the other hand, the kinetics of Na^+ inactivation and of charge immobilization are prolonged (Figs. 3 and 8). The zero-time intercept I'_{Na} of the Na^+ current and the fast 'on' charge displacement Q_{on} are diminished (Fig. 5). The $\tau_m(V)$, $m_\infty^3(V)$ and $Q_{on}(V)$ curves are shifted to the left. These parallelisms support the notion that gating currents indeed arise from reactions in Na^+ channels and that the fast 'on' charge displacement is related to the process of Na^+ activation, while charge immobilization and Na^+ inactivation are linked to each other [30,31].

A quantitative comparison between ATX II effects on the magnitude and kinetics of Na^+ and gating currents is difficult for the following reasons: in our investigation, we have analysed the total charge displacement, whereas the characteristics of Na^+ current are better compared with the inactivating fraction of gating currents [24]. Moreover, the determination of the magnitude Q_{on} and of the time constant τ_{on} of the fast 'on' charge displacement may be biassed by the presence of slower components (see Fig. 6A) which are almost abolished after ATX II application (Fig. 6B). Scorpion toxins also remove such slow components in the 'on' responses of gating currents [25,26]. These similar toxin effects suggest that the slow components under control conditions are no artifacts. It is unlikely that these components are entirely due to asymmetries of ionic currents because ATX II does not only affect the pedestal but also the decaying phase of the 'on' response. Thus, charge displacements from slow gating processes in Na^+ or K^+ channels seem to contribute at least partly to the observed slower components. With scorpion toxins, no decision between these two possibilities could be reached [26] because these toxins slow Na^+ inactivation as well as K^+ activation [32]. ATX II, on the other hand, does not affect the kinetics of K^+ currents [3,5]. The abolishment of slow 'on' charge displacements in ATX II is then most likely due to the prolonged Na^+ inactivation. Hence, Na^+ inactivation seems to contribute some charge displacement during depolarizations in normal nerve fibres as suggested recently for the crayfish axon [33]. An analysis of these slow gating current components should yield more information on the voltage dependence of Na^+ inactivation and the interrelation of this gating process with that of Na^+ activation.

Acknowledgements

This investigation was supported by the Deutsche Forschungsgemeinschaft, SFB 38 "Membranforschung". We thank Professor H. Meves and Dr. T. Plant for reading the manuscript and for helpful comments.

References

1 Catterall, W.A. (1980) Annu. Rev. Pharmacol. Toxicol. 20, 15–43
2 Rathmayer, W. and Beress, L. (1976) J. Comp. Physiol. 109, 373–382
3 Romey, G., Abita, J.P., Schweitz, H., Wunderer, G. and Lazdunski, M. (1976) Proc. Natl. Acad. Sci. USA 73, 4055–4059
4 Warashina, A. and Fujita, S. (1983) J. Gen. Physiol. 81, 305–323
5 Bergman, C., Dubois, J.M., Rojas, E. and Rathmayer, W. (1976) Biochim. Biophys. Acta 455, 173–184
6 Conti, F., Hille, B., Neumcke, B., Nonner, W. and Stämpfli, R. (1976) J. Physiol. 262, 729–742

7 Neumcke, B., Schwarz, W. and Stämpfli, R. (1980) Biochim. Biophys. Acta 600, 456–466
8 Ulbricht, W. and Schmidtmayer, J. (1981) J. Physiol.(Paris) 77, 1103–1111
9 Schmidtmayer, J., Stoye-Herzog, M. and Ulbricht, W. (1982) Pflügers Arch. 394, 313–319
10 Schmidtmayer, J., Stoye-Herzog, M. and Ulbricht, W. (1983) Pflügers Arch. 398, 204–209
11 Rack, M., Meves, H., Béress, L. and Grünhagen, H.H. (1983) Toxicon 21, 231–237
12 Ravens, U. (1976) Naunyn-Schmiedeberg's Arch. Pharmacol. 296, 73–78
13 Alsen, C., Harris, J.B. and Tesseraux, I. (1981) Br. J. Pharmacol. 74, 61–71
14 Schwarz, W. (1983) Experientia 39, 935–941
15 Neumcke, B., Schwarz, W. and Stämpfli, R. (1984) Pflügers Arch. 400, R 37
16 Stämpfli, R. and Hille, B. (1976) in Frog Neurobiology (Llinás, R. and Precht, W., eds.), pp. 3–32, Springer-Verlag, Berlin
17 Nonner, W. (1969) Pflügers Arch. 309, 176–192
18 Sigworth, F.J. (1980) J. Physiol. 307, 97–129
19 Frankenhaeuser, B. (1960) J. Physiol. 151, 491–501
20 Dubois, J.M. and Schneider, M.F. (1982) J. Gen. Physiol. 79, 571–602
21 Nonner, W., Rojas, E. and Stämpfli, R. (1978) Pflügers Arch. 375, 75–85
22 Chiu, S.Y. (1977) J. Physiol. 273, 573–596
23 French, R.J. and Horn, R. (1983) Annu. Rev. Biophys. Bioeng. 12, 319–356
24 Keynes, R.D., Greeff, N.G. and Van Helden, D.F. (1982) Proc. R. Soc. Lond. B 215, 391–404
25 Krutetzkaja, Z., Lonsky, A., Mozhayeva, G. and Naumov, A. (1978) Zytologia 20, 1269–1277
26 Nonner, W. (1979) Adv. Cytopharmacol. 3, 345–352
27 Armstrong, C.M. and Bezanilla, F. (1977) J. Gen. Physiol. 70, 567–590
28 Neumcke, B., Schwarz, W. and Stämpfli, R. (1981) Pflügers Arch. 390, 230–236
29 Bekkers, J.M., Greeff, N.G., Keynes, R.D. and Neumcke, B. (1984) J. Physiol. 352, 653–668
30 Meves, H. (1977) Ann. N. Y. Acad. Sci. 303, 322–338
31 Armstrong, C.M. (1981) Physiol. Rev. 61, 644–683
32 Koppenhöfer, E. and Schmidt, H. (1968) Pflügers Arch. 303, 133–149
33 Swenson, R.P., Jr. (1983) Biophys. J. 41, 245–249